Hindawi
Mathematical Problems in Engineering
Volume 2018, Article ID 6790420, 15 pages
https://doi.org/10.1155/2018/6790420

Research Article

Heat and Mass Transfer in Three-Dimensional Flow of an Oldroyd-B Nanofluid with Gyrotactic Micro-Organisms

M. Sulaiman,[1,2] Aamir Ali ,[1] and S. Islam [2]

[1] *Department of Mathematics, COMSATS University Islamabad, Attock Campus, Attock, 43600, Pakistan*
[2] *Department of Mathematics, Abdul Wali Khan University, Mardan, Khyber Pakhtunkhwa, 23200, Pakistan*

Correspondence should be addressed to Aamir Ali; aamir_ali@ciit-attock.edu.pk

Received 10 December 2017; Revised 28 February 2018; Accepted 29 April 2018; Published 6 September 2018

Academic Editor: Efstratios Tzirtzilakis

This paper discusses the three-dimensional flow of the gyrotactic bioconvection of an Oldroyd-B nanofluid over a stretching surface. Theory of microorganisms is utilized to stabilize the suspended nanoparticles through bioconvection induced by the effects of buoyancy forces. Analytic solution for the governing nonlinear equations is obtained by using homotopy analysis method (HAM). The effects of involved parameters on velocity, temperature, nanoparticles concentration, and density of motile microorganisms are discussed graphically. The local Nusselt, Sherwood, and motile microorganisms numbers are also analyzed graphically. Several known results have been pointed out as the particular cases of the present analysis. It is found that the non-Newtonian fluid parameters, i.e., relaxation time parameter β_1 and retardation time parameter β_2, have opposite effects on the velocity profile. The velocity of the fluid and boundary layer thickness decreases for increasing relaxation time while it decreases for increasing retardation time effects.

1. Introduction

In recent years the significance of the study of non-Newtonian fluids has remarkably increased due to its applications in engineering, industry, and biological sciences, e.g., in material processing, food, and cosmetic industries [1]. These applications generally involve complex geometries and require that the response of the fluid to given temperature conditions is controlled. The basic equations that governs the flow of non-Newtonian fluids are highly nonlinear. The mathematical description of a non-Newtonian fluid requires a constitutive equation that determines the rheological properties of the fluid. Due to the complexity, the aforementioned fluids are generally divided into three types, namely, the differential type, the rate type, and the integral type. The simplest example of rate type fluid is Maxwell fluid model which narrates the properties of relaxation time. But it cannot predict the retardation time effects. The Oldroyd-B fluid is one subclass of the rate type fluid which describes the properties of both the relaxation time and the retardation time. There are several investigations in this direction for two-dimensional flow configurations with different features of the non-Newtonian fluid models [2–10]. However, in practical applications sometimes, the flow is three-dimensional. In view of such motivation, researchers have studied the three-dimensional flow for different flow geometries (see ref. [11–17]).

The problem of heat and mass transfer analysis over a stretched boundary layer is of great interest to researchers due to its engineering and industrial applications like glass fiber, manufacture and drawing of plastics and rubber sheets, paper production, cooling of continuous stripes and an infinite metallic sheet, the continuous casting, polymer extrusion process, heat treated materials travelling on conveyer belts, food processing, and many others. Sakiadis [18] has done the pioneer work in the analysis of the boundary layer flow on a moving surface, which was later extended by Crane [19] by considering the linearly stretching surface. Rashad and Kabeir [20] studied the heat and mass transfer in transient flow by mixed convection boundary layer over a stretching sheet embedded in a porous medium with chemically reactive species. Sandeep and Sulochana [21] studied the generalized model for momentum and heat transfer behavior of Jeffrey, Maxwell, and Oldroyd-B nanofluids over a stretching

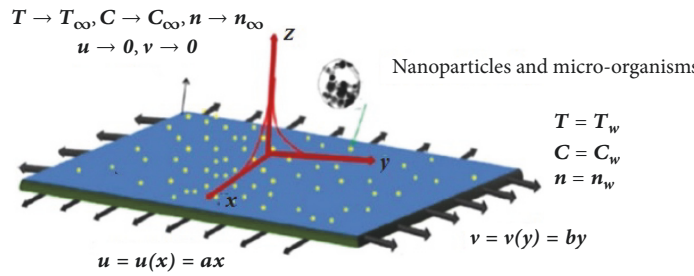

Figure 1: Geometry of the problem.

surface with nonuniform heat source/sink. After that, several investigations have been done by considering different flow configurations [22–28].

With the advent of nanoscience, nanofluids have become a focus of attention in the study of fluid flow in the presence of nanoparticles. Nanofluids can be used to increase the thermal conductivity of the fluids and are stable fluids having much better writing, dispersion, and spreading properties on solid surfaces. Choi and Eastman [29] initially presented the idea of suspension of nanoparticles in base fluids. Later, Buongiorno [30] extended the concept by considering Brownian motion and thermophoresis movement of nanoparticles in view of application in hybrid power engine, thermal management, heat exchanger, domestic refrigerators, etc. They have enhanced heat conduction power as compared to base fluids and are useful in cancer therapy and medicine. With the presentation of a reliable model of nanofluid given by Buongiorno [30], nanofluids have become a subject of great interest for researchers in the last few decades [31–34]. Recently, Nabwey et al. [35] studied the group method analysis of mixed convection stagnation-point flow of non-Newtonian nanofluid over a vertical stretching surface.

Bioconvection is a phenomenon that is used to describe the unstructured pattern and instability produced by the microorganisms, which are swimming to the upper part of a fluid and has a lesser density. Due to swimming upwards, these involved microorganisms such as gyrotactic microorganisms like algae tend to concentrate in the upper part of the fluid layer, causing unstable top heavy density stratification (see [36]). Nanofluid bioconvection phenomenon describes the unstructured density stratification and formation of patterns due to synchronized interaction of the nanoparticles, thicker self-propelled microorganisms and buoyancy forces. Brownian motion and thermophoresis effect produce the motion of these particles, which is independent of the movement of motile microorganisms. That is why the combined interface of bioconvection and nanofluids becomes significant for microfluidic appliances. Uddin et al. studied the computational investigation of Stefan blowing and multiple-slip effects on buoyancy-driven bioconvection nanofluid flow with microorganisms [37] and numerical solutions for gyrotactic bioconvection in nanofluid saturated porous media with Stefan blowing and multiple slip effects [38]. Different types of microorganisms, theoretical biconvection models, have been studied [39–51].

In present study, we have entered a new concept in the problem of boundary layer flow passing a stretching sheet. We have considered the three-dimensional bioconvection flow of an Oldroyd-B nanofluid which contains self-impelled motile gyrotactic microorganisms, over a bidirectional stretching surface. This work is an extension of the work of W. A. Khan et al. [16] by considering the gyrotactic microorganisms in the three-dimensional flow of Oldroyd-B nanofluid. The problem is formulated in terms of governing equations of motion with appropriate boundary conditions, which are then transformed into a system of ordinary differential equations using similarity transformations. The analytical solution is found using Homotopy Analysis Methods (HAM). The effects of involved physical parameters on the flow fields are analyzed with the help of graphs.

2. Problem Formulation

We have considered the steady, incompressible three-dimensional flow of an Oldroyed-B nanofluid containing gyrotactic microorganisms past a stretching surface. The surface is maintained at constant temperature T_w, the nanoparticle volume fraction C_w, and the number of motile microorganisms n_w; the ambient values of temperature, nanoparticle volume fraction, and number of motile microorganisms are denoted by T_∞, C_∞, and n_∞, respectively, while the reference values are by T_0, C_0, and n_0, respectively. The microorganisms are taken into the nanofluid to stabilize the nanoparticles due to bioconvection. The mechanical analog for the Oldroyd-B model and the geometry of the present analysis is shown in Figure 1. The boundary layer form of the continuity, momentum, energy, nanoparticle concentration, and density of microorganisms for three-dimensional Oldroyd-B fluid is as follows ([16, 37, 50]):

$$\frac{\partial u}{\partial x} + \frac{\partial v}{\partial y} + \frac{\partial w}{\partial z} = 0, \tag{1}$$

$$u\frac{\partial u}{\partial x} + v\frac{\partial u}{\partial y} + w\frac{\partial u}{\partial z} + \lambda_1\left(u^2\frac{\partial^2 u}{\partial x^2} + v^2\frac{\partial^2 u}{\partial y^2} + w^2\frac{\partial^2 u}{\partial z^2} + 2uv\frac{\partial^2 u}{\partial x\partial y} + 2vw\frac{\partial^2 u}{\partial y\partial z} + 2uw\frac{\partial^2 u}{\partial x\partial z}\right) = \nu\left[\frac{\partial^2 u}{\partial z^2} + \lambda_2\left(u\frac{\partial^3 u}{\partial x\partial z^2} + v\frac{\partial^3 u}{\partial y\partial z^2} + w\frac{\partial^3 u}{\partial z^3} - \frac{\partial u}{\partial x}\frac{\partial^2 u}{\partial z^2}\right.\right.$$

$$-\frac{\partial u}{\partial y}\frac{\partial^2 v}{\partial z^2}-\frac{\partial u}{\partial z}\frac{\partial^2 w}{\partial z^2}\Bigg)\Bigg]+\frac{1}{\rho_f}\left[\rho_f\beta\left(1-C_\infty\right)\left(T-T_\infty\right)-\left(\rho_p-\rho_f\right)\left(C-C_\infty\right)-\gamma\left(\rho_m-\rho_f\right)\left(n-n_\infty\right)\right]\mathrm{g}, \tag{2}$$

$$u\frac{\partial v}{\partial x}+v\frac{\partial v}{\partial y}+w\frac{\partial v}{\partial z}+\lambda_1\left(u^2\frac{\partial^2 v}{\partial x^2}+v^2\frac{\partial^2 v}{\partial y^2}+w^2\frac{\partial^2 v}{\partial y^2}\cdot+2uv\frac{\partial^2 v}{\partial x\partial y}+2vw\frac{\partial^2 v}{\partial y\partial z}+2uw\frac{\partial^2 v}{\partial x\partial z}\right)=\nu\left[\frac{\partial^2 v}{\partial z^2}+\lambda_2\left(u\frac{\partial^3 u}{\partial x\partial z^2}+v\frac{\partial^3 u}{\partial y\partial z^2}+w\frac{\partial^3 u}{\partial z^3}-\frac{\partial u}{\partial x}\frac{\partial^2 u}{\partial z^2}-\frac{\partial u}{\partial y}\frac{\partial^2 v}{\partial z^2}-\frac{\partial u}{\partial z}\frac{\partial^2 w}{\partial z^2}\right)\right], \tag{3}$$

$$u\frac{\partial T}{\partial x}+v\frac{\partial T}{\partial y}+w\frac{\partial T}{\partial z}=\alpha_m\frac{\partial^2 T}{\partial z^2}+\tau\left[D_B\left(\frac{\partial C}{\partial z}\frac{\partial T}{\partial z}\right)+\frac{D_T}{T_\infty}\left(\frac{\partial T}{\partial z}\right)^2\right], \tag{4}$$

$$u\frac{\partial C}{\partial x}+v\frac{\partial C}{\partial y}+w\frac{\partial C}{\partial z}=D_B\frac{\partial^2 C}{\partial z^2}+\frac{D_T}{T_\infty}\left(\frac{\partial^2 T}{\partial z^2}\right), \tag{5}$$

$$u\frac{\partial n}{\partial x}+v\frac{\partial n}{\partial y}+w\frac{\partial n}{\partial z}+\frac{bw_0}{\Delta C}\left[\frac{\partial}{\partial z}\left(n\frac{\partial C}{\partial z}\right)\right]=D_m\frac{\partial^2 n}{\partial z^2}, \tag{6}$$

and the boundary conditions are as follows:

$$\begin{aligned}
&u=u_w(x)=U_w=ax,\\
&v=v_w(y)=V_w=by,\\
&w=0,\\
&T=T_w=T_0+b_1x,\\
&C=C_w=C_0+d_1x,\\
&n=n_w=n_0+e_1x,\\
&\qquad\qquad\text{at } z=0,\\
&u\longrightarrow 0,\\
&v\longrightarrow 0,\\
&T\longrightarrow T_\infty,\\
&C\longrightarrow C_\infty,\\
&n\longrightarrow n_\infty\\
&\qquad\qquad\text{as } z\longrightarrow\infty,
\end{aligned} \tag{7}$$

in which u, v, and w are the velocity components in the x, y, and z directions, respectively, ν is the kinematic viscosity, λ_1 and λ_2 are the relaxation time and retardation time, ρ_f is the density of nanofluid, ρ_p is the density of nanoparticles, ρ_m is the density of microorganisms particles, g is the gravity, $\tau=(\rho c)_p/(\rho c)_f$ is the heat capacity ratio, U_w and V_w are the stretching velocities, $a,b>0$ are the stretching rate, and b_1,d_1,e_1 are the dimensional constant. Let us introduce the following transformations:

$$\begin{aligned}
\eta&=\sqrt{\frac{a}{\nu}}z,\\
u&=axf'(\eta),\\
v&=ayg'(\eta),\\
w&=-\sqrt{a\nu}\left[f(\eta)+g(\eta)\right],\\
\theta(\eta)&=\frac{T-T_\infty}{T_w-T_0},\\
\phi(\eta)&=\frac{C-C_\infty}{C_w-C_0},\\
N(\eta)&=\frac{n-n_\infty}{n_w-n_0},
\end{aligned} \tag{8}$$

The continuity (1) is identically satisfied and (2) to (6) takes the following forms:

$$\begin{aligned}
&f'''+(f+g)f''-f'^2\\
&\quad+\beta_1\left[2(f+g)f'f''-(f+g)^2f'''\right]\\
&\quad+\beta_2\left[2\left(f''+g''\right)f''-(f+g)f^{iv}\right]\\
&\quad+\lambda\left(\theta-Nr\phi-RbN\right)=0,
\end{aligned} \tag{9}$$

$$\begin{aligned}
&g'''+(f+g)g''-g'^2\\
&\quad+\beta_1\left[2(f+g)g'g''-(f+g)^2g'''\right]\\
&\quad+\beta_2\left[2\left(f''+g''\right)g''-(f+g)g^{iv}\right]=0,
\end{aligned} \tag{10}$$

$$\theta''+Pr(f+g)\theta'-Prf'\theta+N_b\phi'\theta'+N_t\left(\theta'\right)^2=0, \tag{11}$$

$$\phi''+Le(f+g)\phi'-Lef'\phi+\frac{N_t}{N_b}\theta''=0, \tag{12}$$

$$\begin{aligned}
&N''+Lb(f+g)N'-Lbf'N\\
&\quad-Pe\left[\phi'N'+(N+\Omega)\phi''\right]=0,
\end{aligned} \tag{13}$$

and the boundary conditions (7) is reduced to the following:

$$\begin{aligned}
f(0)&=0,\\
g(0)&=0,\\
f'(0)&=1,
\end{aligned}$$

$$
\begin{aligned}
g'(0) &= \alpha,\\
\theta(0) &= 1,\\
\phi(0) &= 1,\\
N(0) &= 1,\\
f'(\infty) &= 0,\\
g'(\infty) &= 0,\\
\theta(\infty) &\longrightarrow 0,\\
\phi(\infty) &\longrightarrow 0,\\
N(\infty) &\longrightarrow 0,
\end{aligned}
\tag{14}
$$

where prime is the differentiation with respect to η. Furthermore, β_1, β_2, λ, Nr, Rb, Pr, Nb, Nt, Le, Lb, Pe, Ω, and α are the Deborah number, the mixed convection parameter, the buoyancy ratio parameter, the bioconvection Rayleigh number, the Prandtl number, the Brownian motion parameter, the thermophoresis parameter, the Lewis number, the bioconvection Lewis number, the bioconvection Peclet number, the microorganisms concentration difference parameter, and stretching ratio parameter which are the nondimensional parameters and are defined as follows:

$$
\begin{aligned}
\beta_1 &= \lambda_1 a,\\
\beta_2 &= \lambda_2 b,\\
\lambda &= \frac{g\beta\rho_f\left(1-C_\infty\right)\left(T_w-T_0\right)\left(x^3/\nu^2\right)}{U_w^2\left(x^2/\nu^2\right)} = \frac{Gr_x}{Re_x^2},\\
Nr &= \frac{\left(\rho_p-\rho_f\right)\left(C_w-C_0\right)}{\rho_f\left(1-C_\infty\right)\left(T_w-T_0\right)\beta},\\
Rb &= \frac{\gamma\left(\rho_m-\rho_f\right)\left(n_w-n_0\right)g}{\rho_f\left(1-C_\infty\right)\left(T_w-T_0\right)\beta},\\
Pr &= \frac{\nu}{\alpha_m},\\
N_b &= \tau D_B\frac{\left(C_w-C_0\right)}{\alpha_m},\\
N_t &= \tau D_T\frac{\left(T_w-T_0\right)}{\alpha_m T_\infty},\\
Le &= \frac{\nu}{D_B},\\
Lb &= \frac{\nu}{D_{m_0}},\\
Pe &= \frac{b\omega_{m_0}}{D_{m_0}},
\end{aligned}
$$

$$
\begin{aligned}
\Omega &= \frac{n_\infty}{n_w-n_0},\\
\alpha &= \frac{b}{a}.
\end{aligned}
\tag{15}
$$

The nondimensional ordinary differential (9)-(13) subject to the boundary conditions (14) are solved analytically by using homotopy analysis method (HAM). HAM technique was first introduced by Liao [52] in his Ph.D. thesis. He devised a parameter that controls convergence of the series solution. The method has been successfully applied in the literature to compute analytic solution of various problems ([53–56] and references therein). The details of the method are given in the appendix. Homotopy analysis method ensures the convergence of derived series solution. The auxiliary parameter h plays a vital role in controlling and adjusting the convergence region of series solutions. We have plotted the h–curves shown in Figure 2 and found that the admissible values of auxiliary parameters $h_f, h_g, h_\theta, h_\phi$ and h_N are $-1.45 \le h_f \le -0.05$, $-1.25 \le h_g \le -0.1$, $-1.45 \le h_\theta \le -0.05$, $-1.3 \le h_\phi \le -0.15$, and $-1.5 \le h_N \le -0.2$, respectively. The expressions for local Nusselt number, local Sherwood number, and local density number of the motile microorganisms are defined as follows:

$$
\begin{aligned}
Nu &= \frac{xq_w}{k\left(T_w-T_0\right)},\\
Sh &= \frac{xq_m}{D_B\left(C_w-C_0\right)},\\
Nn &= \frac{xq_n}{D_n\left(n_w-n_0\right)},
\end{aligned}
\tag{16}
$$

where

$$
\begin{aligned}
q_w &= \left(-k\frac{\partial T}{\partial z}\right)_{z=0},\\
q_m &= \left(-D_B\frac{\partial C}{\partial z}\right)_{z=0},\\
q_n &= \left(-D_m\frac{\partial n}{\partial z}\right)_{z=0}.
\end{aligned}
\tag{17}
$$

The dimensionless forms of local Nusselt number, local Sherwood number, and local motile microorganism are as follows

$$
\begin{aligned}
NuRe_x^{-1/2} &= -\theta'(0),\\
ShRe_x^{-1/2} &= -\phi'(0),\\
NnRe_x^{-1/2} &= -N'(0),
\end{aligned}
\tag{18}
$$

where $Re_x = xU_w/\nu$ is the Reynolds number.

3. Results and Discussion

This section explores the results of three-dimensional flow of an Oldroyed-B nanofluid over a stretching sheet in the

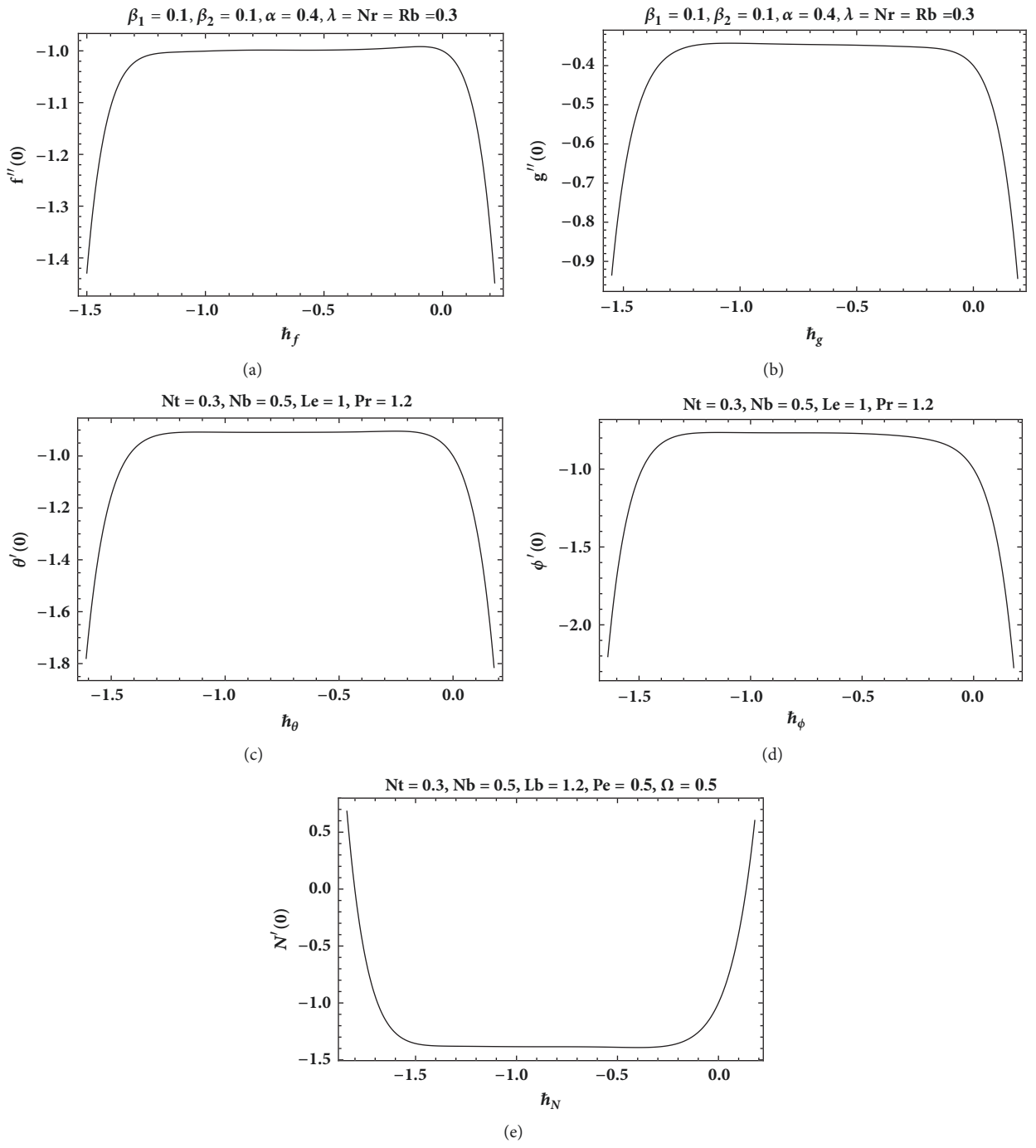

FIGURE 2: h–curves for (a) f, (b) g, (c) θ, (d) ϕ, and (e) N.

presence of gyrotactic micr-organisms. The analytic results for the problem are presented graphically to study the behavior of some physical parameters on the velocities f', g', temperature θ, concentration of nanoparticles ϕ, and concentration of microorganisms N. In Figure 3, the effects of Deborah numbers β_1 and β_2 on the velocity component f' are examined for fixed values of other parameters. The opposite behavior of velocity profile is observed for increasing values of β_1 and β_2. Nonzero values of β_1 and β_2 correspond to elastic effects which retards the flow and hence the boundary layer will be thinner which is noted. The similar behavior for β_1 and β_2 can be observed for the velocity component g' in Figure 4.

The influence of stretching ratio parameter α on the velocity component g' is shown in Figure 5. It is observed that when the values of α are increased the velocity at the wall, $\eta = 0$ is increased.

In Figure 6, the impact of (a) bioconvection Rayleigh number Rb and (b) buoyancy ratio parameter Nr on the velocity component f' is shown. The graphical results show

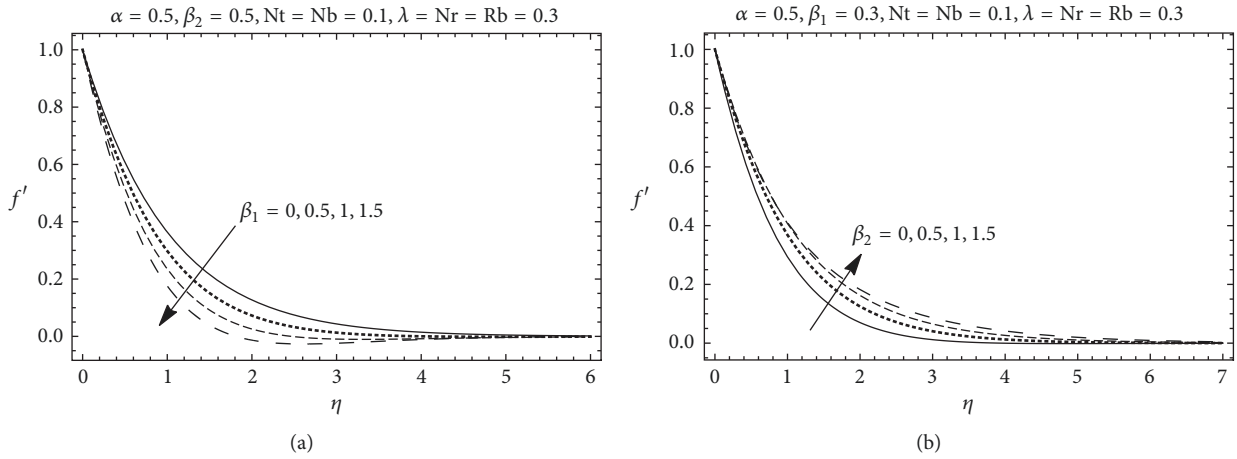

Figure 3: Influence of (a) β_1 (b) β_2 on f'.

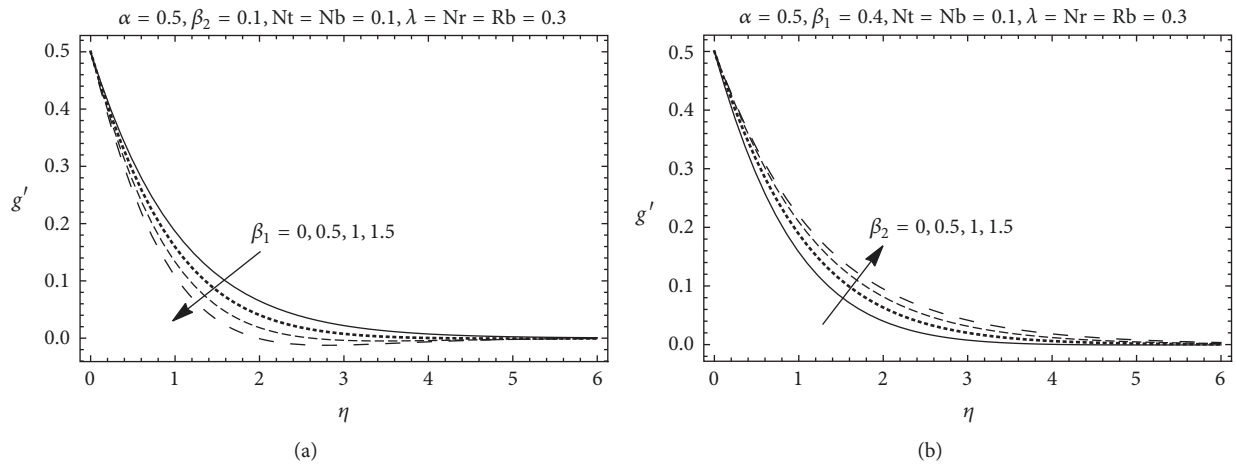

Figure 4: Influence of (a) β_1 (b) β_2 on g'.

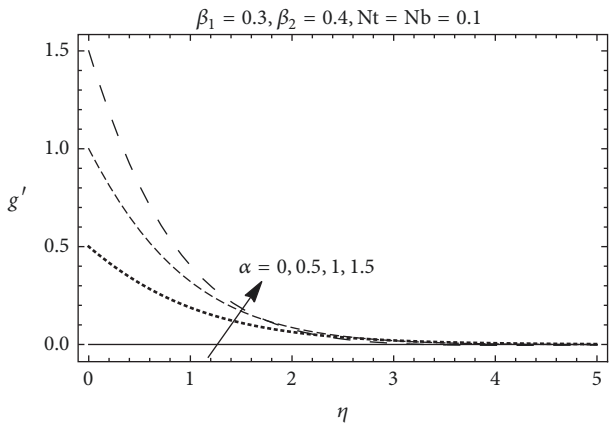

Figure 5: Influence of stretching ratio α on velocity component g'.

that when the values of Rb and Nr are increasing, a rapid decrease in the velocity profile is observed.

The combined effects of the thermophoresis parameter Nt and Brownian motion parameter Nb on the temperature profile are shown in Figure 7(a). The temperature profile increases when we increase the values of Nt and Nb, since increasing the magnitude of Brownian motion on the particles and thermal diffusivity of the nanoparticles will accelerate the temperature of the nanofluid. The impact of Prandtl number Pr on temperature profile is shown in Figure 7(b). The increasing values of Prandtle number decrease the temperature of the system. Figure 7(b) clearly depicts that the larger value of Prandtl number Pr corresponds to the lower heat and thermal boundary layer thickness. The Prandtl number indeed plays an essential role in heat transfer; it controls the relative thickness of the thermal boundary layer. In order to characterize the mixed convection flow, it is also important to investigate the effect of the Prandtl number on the temperature profile. We observe that the temperature decreases with increasing Prandtl number. This may be explained by the fact that increasing the Prandtl number is equivalent to reducing the thermal diffusivity, which characterizes the rate at which heat is conducted.

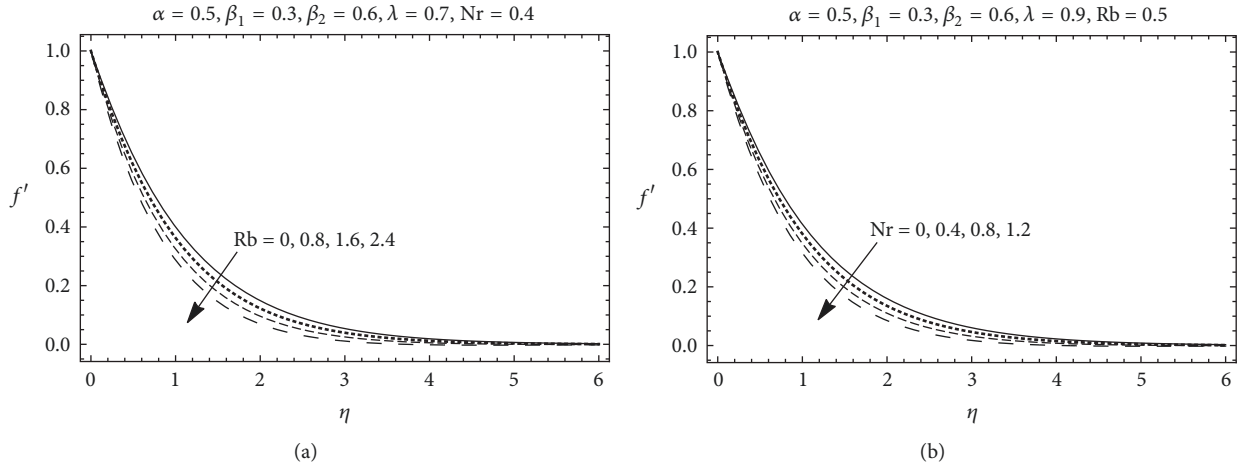

Figure 6: Influence of (a) Rb (b) Nr on f'.

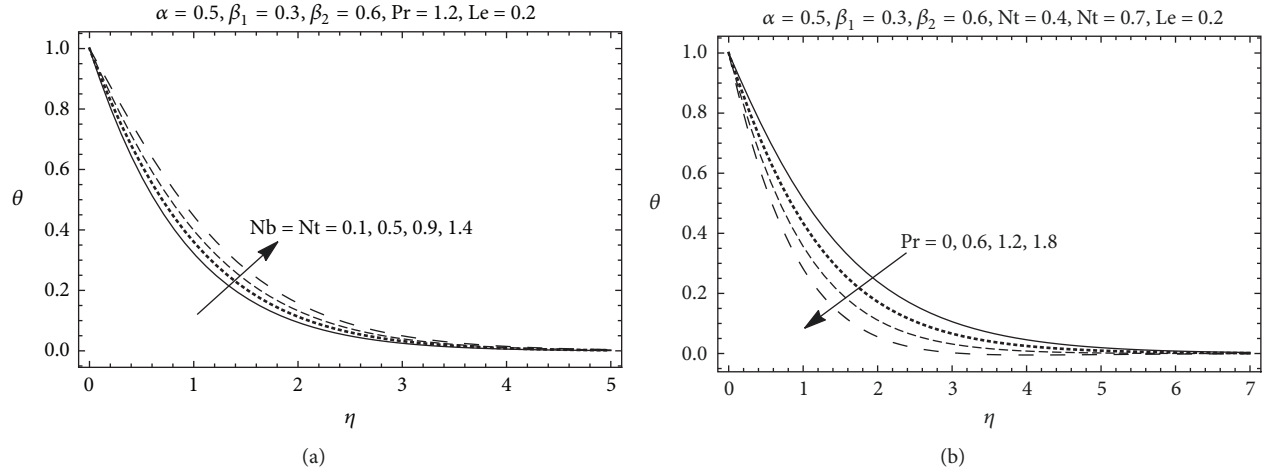

Figure 7: Influence of (a) Nb and Nt (b) Pr on θ.

To analyze the concentration ϕ of the nanoparticles, the values of Brownian diffusion parameter and thermophoresis diffusion parameter are varied for fixed values of other parameters as shown in Figure 8(a); for larger values of Nt and Nb, the concentration profile ϕ increases. Increase in the values of Nt and Nb refers to increase in number of nanoparticles. Thus higher concentration of nanoparticles corresponds to higher Brownian and thermophoresis diffusion which can also be seen from Figure 8(a). The effect of Lewis number can be seen in Figure 8(b). If we increase the value of Lewis number, the concentration of the nanoparticle decreases.

The influence of dimensionless bioconvection Lewis number Lb on concentration of microorganisms N is shown in Figure 9(a). The graphs illustrate a rapid decline in the profile, because the bioconvection Lewis number opposes the motion of the fluid. The relation of microorganisms concentration difference parameter Ω and motile density of the microorganisms N is discussed in Figure 9(b). For higher values of Ω, a decrease noticed in the value of N.

The effects of Peclet number Pe on N are shown in Figure 10, which shows the buoyancy parameter is found to be more pronounced for a fluid with greater values of bioconvection Péclet number Pe.

Numerical values for $-f''(0)$ and $-g''(0)$ are compared with the existing literature in the absence of non-Newtonian effects are shown in Table 1, and an excellent agreement has been found, which validate the present results. The numerical values of local Nusselt number, local Sherwood number, and local density of motile microorganisms are presented in Table 2 for different values of α, λ, Nb, Nt, and Ω. We can observe that the magnitude of local Nusselt number is increased by increasing α and λ while it decreased by increasing Nb and Nt. In other words, heat flux at the surface is a decreasing function of nanoparticle properties. In other words, heat flux at the surface reduces in the presence of nanoparticles and can be controlled by varying the quantity and quality of nanoparticles. Similarly, the magnitude of local Sherwood number and local density of motile microorganisms is increasing by increasing values

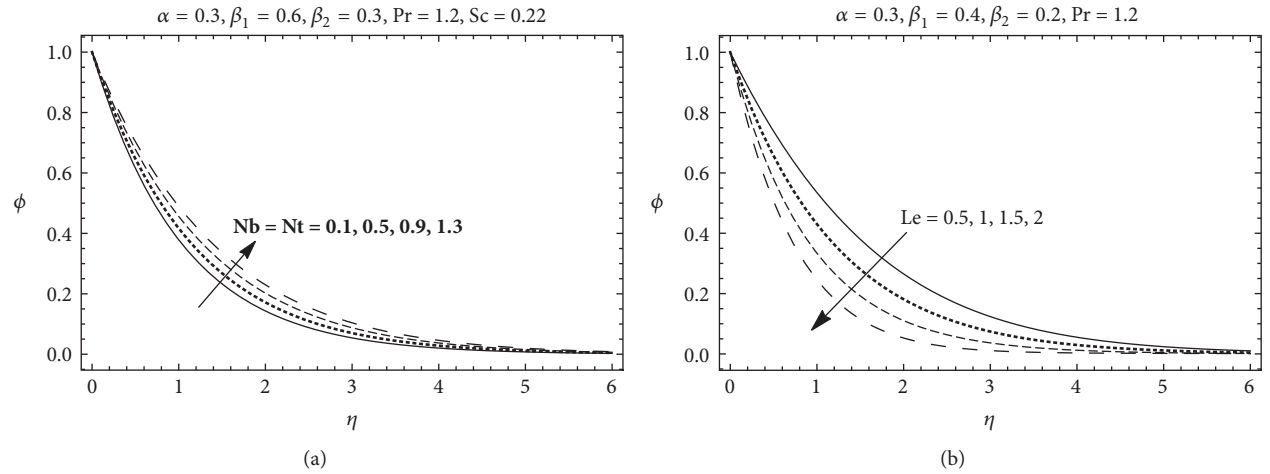

Figure 8: Influence of (a) Nb and Nt (b) Le on ϕ.

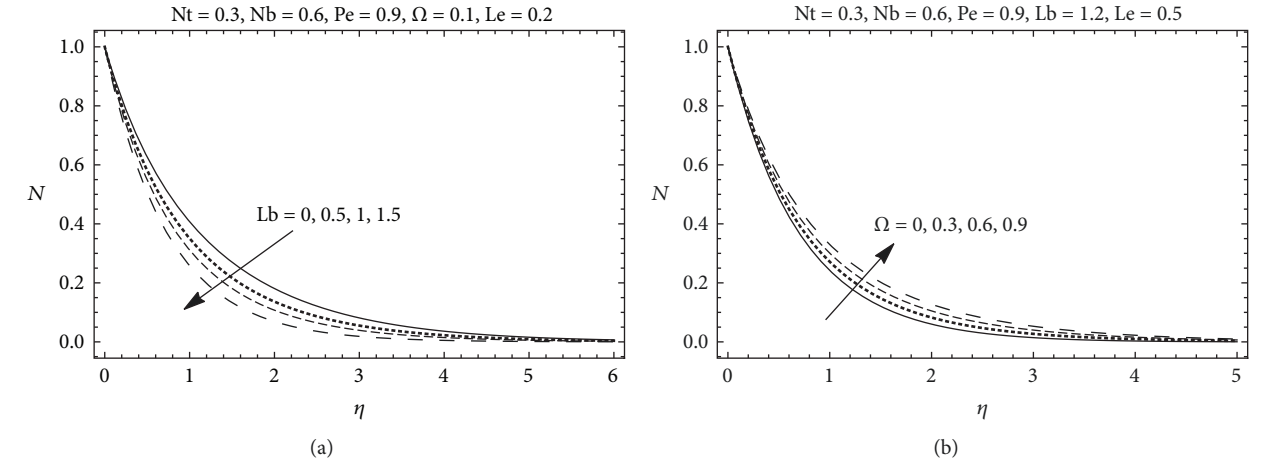

Figure 9: Influence of (a) Nb and Nt (b) Ω on N.

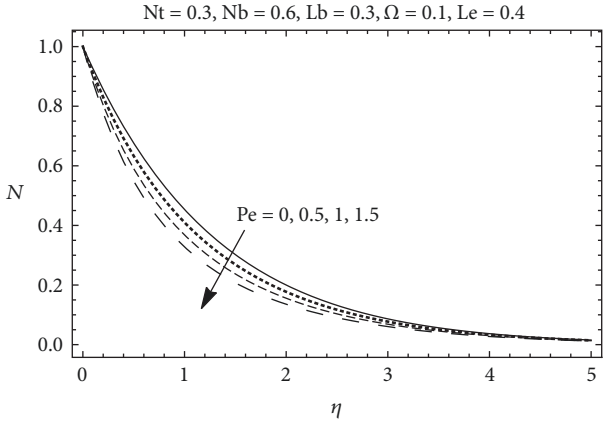

Figure 10: Influence of Pe on N.

of α, λ, and Nb while it decreases for increasing Nt. In other words, local Sherwood number and local density of motile microorganisms are decreasing function of both the thermophoretic diffusion and Brownian diffusion parameter for all values of other parameters.

4. Concluding Remarks

In this paper, we have discussed the three-dimensional bioconvection flow of an Oldroyd-B nanofluid over a stretching surface with gyrotactic microorganisms. Analytic technique is applied to investigate the problem and series solution is computed by using homotopy analysis method. The velocity, temperature, concentration, and microorganisms profiles are plotted to analyze the effects of various physical parameters. The main observations are as follows:

(i) The Deborah number β_1 decreases the velocity profile, while β_2 increases the velocity profile.

(ii) The velocity component f' decreases for increasing values of Rb and Nr.

(iii) The stretching ratio parameter α increases the velocity component g'.

Table 1: Comparison for the velocity gradient for different values of α when $\beta_1 = \beta_2 = 0$.

	$-f''(0)$			$-g''(0)$		
α	HPM result [15]	Exact result [15]	Present result	HPM result [15]	Exact result [15]	Present result
0.0	1.0	1.0	1.0	0	0	0
0.1	1.02025	1.020259	1.020253	0.06684	0.066847	0.066849
0.2	1.03949	1.039495	1.039498	0.14873	0.148736	0.148730
0.3	1.05795	1.05794	1.057959	0.24335	0.243359	0.243360
0.4	1.07578	1.075788	1.075789	0.34920	0.349208	0.349212
0.5	1.09309	1.093095	1.093093	0.46520	0.465204	0.465206
0.6	1.10994	1.109946	1.109944	0.59052	0.590528	0.590527
0.7	1.12639	1.126397	1.126396	0.72453	0.724531	0.724529
0.8	1.14248	1.142488	1.142489	0.86668	0.866682	0.866683
0.9	1.15825	1.158253	1.158256	1.01653	1.016538	1.016541
1.0	1.17372	1.17372	1.173723	1.17372	1.173720	1.173723

Table 2: Numerical values of local Nusselt number $NuRe_x^{-1/2}$, local Sherwood number $ShRe_x^{-1/2}$, and local density of motile microorganisms $NnRe_x^{-1/2}$ for different values of α, λ, Nb, Nt, and Ω.

α	λ	Nb	Nt	Ω	$-\theta'(0)$	$-\phi'(0)$	$-N'(0)$
0.0	0.2	0.3	0.3	0.2	0.861666	0.522014	1.024791
0.5					0.929823	0.571493	1.118607
1.0					1.002058	0.634386	1.227815
0.5	0.0	0.3	0.3	0.2	0.918579	0.554933	1.104269
	0.5				0.943804	0.592014	1.136527
	1.0				0.960169	0.616448	1.158511
0.5	0.3	0.1	0.3	0.2	1.010617	−0.700285	1.129376
		0.5			0.864386	0.832249	1.125671
		0.9			0.738619	0.997418	1.127016
0.5	0.3	0.3	0	0.2	0.998064	1.124014	1.124014
			0.5		0.896472	0.263520	1.125716
			1.0		0.812228	−0.390333	1.127555
0.5	0.2	0.3	0.3	0	0.929823	0.571493	1.118607
				0.5	0.929823	0.571493	1.118607
				1.0	0.929823	0.571493	1.118607

(iv) The combined effects of Brownian diffusion parameter Nb and thermophoretic diffusion parameter Nt decrease the temperature and concentration profiles.

(v) The Prandtl number Pr and Schmidt number Sc also decrease the temperature and concentration profiles.

(vi) The concentration of microorganism N has decreasing behavior for increasing Lb, Pe, and $Omega$.

(vii) The local Nusselt number and local Sherwood number are decreasing functions of nanoparticle properties.

(viii) The density of motile microorganisms is an increasing function of bioconvection Lewis number and bioconvection Peclet number.

Appendix

A. Homotopy Analysis Method (HAM)

The initial guesses and auxiliary linear operators for the dimensionless momentum, energy, concentration of nanoparticles, and concentration of motile microorganisms equations are denoted by $f_0, g_0, \theta_0, \phi_0, N_0$ and $\mathfrak{L}_f, \mathfrak{L}_g, \mathfrak{L}_\theta, \mathfrak{L}_\phi, \mathfrak{L}_N$ and are defined as follows:

$$\begin{aligned} f_0(\eta) &= 1 - \exp(-\eta), \\ g_0(\eta) &= \alpha[1 - \exp(-\eta)] \\ \theta_0(\eta) &= \exp(-\eta), \\ \phi_0(\eta) &= \exp(-\eta), \\ N_0(\eta) &= \exp(-\eta), \end{aligned} \tag{A.1}$$

and

$$\begin{aligned}
\mathfrak{L}_f &= \frac{d^3 f}{d\eta^3} - \frac{df}{d\eta}, \\
\mathfrak{L}_g &= \frac{d^3 g}{d\eta^3} - \frac{dg}{d\eta}, \\
\mathfrak{L}_\theta &= \frac{d^2\theta}{d\eta^2} - \theta, \\
\mathfrak{L}_\phi &= \frac{d^2\phi}{d\eta^2} - \phi, \\
\mathfrak{L}_N &= \frac{d^2 N}{d\eta^2} - N,
\end{aligned} \tag{A.2}$$

with

$$\begin{aligned}
\mathfrak{L}_f \left[A_1 + A_2 \exp\eta + A_3 \exp -\eta\right] &= 0, \\
\mathfrak{L}_g \left[A_4 + A_5 \exp\eta + A_6 \exp -\eta\right] &= 0, \\
\mathfrak{L}_\theta \left[A_7 \exp\eta + A_8 \exp -\eta\right] &= 0, \\
\mathfrak{L}_\phi \left[A_9 \exp\eta + A_{10} \exp -\eta\right] &= 0, \\
\mathfrak{L}_N \left[A_{11} \exp\eta + A_{12} \exp -\eta\right] &= 0,
\end{aligned} \tag{A.3}$$

where A_i $(i = 1 - 12)$ are the arbitrary constant. The zeroth and m-th order deformation problems are as follows.

A.1. Zeroth-Order Problem

$$\begin{aligned}
&(1-p)\,\mathfrak{L}_f\left[\widehat{f}(\eta,p) - f_0(\eta)\right] = p h_f \mathfrak{N}_f\left[\widehat{f}(\eta,p),\right. \\
&\quad \left.\widehat{g}(\eta,p), \widehat{\theta}(\eta,p), \widehat{\phi}(\eta,p), \widehat{N}(\eta,p)\right], \\
&(1-p)\,\mathfrak{L}_g\left[\widehat{g}(\eta,p) - g_0(\eta)\right] = p h_g \mathfrak{N}_g\left[\widehat{g}(\eta,p),\right. \\
&\quad \left.\widehat{f}(\eta,p), \widehat{\theta}(\eta,p), \widehat{\phi}(\eta,p)\right], \\
&(1-p)\,\mathfrak{L}_\theta\left[\widehat{\theta}(\eta,p) - \theta_0(\eta)\right] = p h_\theta \mathfrak{N}_\theta\left[\widehat{\theta}(\eta,p),\right. \\
&\quad \left.\widehat{f}(\eta,p), \widehat{g}(\eta,p), \widehat{\phi}(\eta,p)\right], \\
&(1-p)\,\mathfrak{L}_\phi\left[\widehat{\phi}(\eta,p) - \phi_0(\eta)\right] = p h_\phi \mathfrak{N}_\phi\left[\widehat{\phi}(\eta,p),\right. \\
&\quad \left.\widehat{f}(\eta,p), \widehat{g}(\eta,p), \widehat{\theta}(\eta,p)\right], \\
&(1-p)\,\mathfrak{L}N\left[\widehat{N}(\eta,p) - N_0(\eta)\right] \\
&\quad = p h_N \mathfrak{N}_N\left[\widehat{N}(\eta,p), \widehat{f}(\eta,p), \widehat{g}(\eta,p), \widehat{\phi}(\eta,p)\right],
\end{aligned} \tag{A.4}$$

with

$$\begin{aligned}
\widehat{f}(0,p) &= 0, \\
\widehat{f}'(0,p) &= 1, \\
\widehat{f}'(\infty,p) &= 0, \\
\widehat{g}(0,p) &= 0, \\
\widehat{g}'(0,p) &= \alpha, \\
\widehat{g}'(\infty,p) &= 0, \\
\widehat{\theta}(0,p) &= 1, \\
\widehat{\theta}(\infty,p) &= 0, \\
\widehat{\phi}(0,p) &= 1, \\
\widehat{\phi}(\infty,p) &= 0, \\
\widehat{N}(0,p) &= 1, \\
\widehat{N}(\infty,p) &= 0,
\end{aligned} \tag{A.5}$$

and

$$\begin{aligned}
&\mathfrak{N}_f\left[\widehat{f}(\eta,p), \widehat{g}(\eta,p), \widehat{\theta}(\eta,p), \widehat{\phi}(\eta,p), \widehat{N}(\eta,p)\right] \\
&\quad = \frac{\partial^3 \widehat{f}(\eta,p)}{\partial\eta^3} + \left(\widehat{f}(\eta,p) + \widehat{g}(\eta,p)\right)\frac{\partial^2 \widehat{f}(\eta,p)}{\partial\eta^2} \\
&\quad - \left(\frac{\partial \widehat{f}(\eta,p)}{\partial\eta}\right)^2 + \beta_1\left[2\left(\widehat{f}(\eta,p)\right.\right. \\
&\quad \left.\left. + \widehat{g}(\eta,p)\right)\frac{\partial \widehat{f}(\eta,p)}{\partial\eta}\frac{\partial^2 \widehat{f}(\eta,p)}{\partial\eta^2}\right. \\
&\quad \left. - \left(\widehat{f}(\eta,p) + \widehat{g}(\eta,p)\right)^2 \frac{\partial^3 \widehat{f}(\eta,p)}{\partial\eta^3}\right] \\
&\quad + \beta_2\left[2\left(\frac{\partial^2 \widehat{f}(\eta,p)}{\partial\eta^2} + \frac{\partial^2 \widehat{g}(\eta,p)}{\partial\eta^2}\right)\frac{\partial^2 \widehat{f}(\eta,p)}{\partial\eta^2}\right. \\
&\quad \left. - \left(\widehat{f}(\eta,p) + \widehat{g}(\eta,p)\right)\frac{\partial^4 \widehat{f}(\eta,p)}{\partial\eta^4}\right] + \lambda\left[\widehat{\theta}(\eta,p)\right. \\
&\quad \left. - Nr\widehat{\phi}(\eta,p) - Rb\widehat{N}(\eta,p)\right], \\
&\mathfrak{N}_g\left[\widehat{g}(\eta,p), \widehat{f}(\eta,p), \widehat{\theta}(\eta,p), \widehat{\phi}(\eta,p)\right] \\
&\quad = \frac{\partial^3 \widehat{g}(\eta,p)}{\partial\eta^3} + \left(\widehat{f}(\eta,p) + \widehat{g}(\eta,p)\right)\frac{\partial^2 \widehat{g}(\eta,p)}{\partial\eta^2} \\
&\quad - \left(\frac{\partial \widehat{g}(\eta,p)}{\partial\eta}\right)^2 + \beta_1\left[2\left(\widehat{f}(\eta,p)\right.\right. \\
&\quad \left.\left. + \widehat{g}(\eta,p)\right)\frac{\partial \widehat{g}(\eta,p)}{\partial\eta}\frac{\partial^2 \widehat{g}(\eta,p)}{\partial\eta^2}\right. \\
&\quad \left. - \left(\widehat{f}(\eta,p) + \widehat{g}(\eta,p)\right)^2 \frac{\partial^3 \widehat{g}(\eta,p)}{\partial\eta^3}\right]
\end{aligned} \tag{A.6}$$

$$+\beta_2\left[2\left(\frac{\partial^2\widehat{f}(\eta,p)}{\partial\eta^2}+\frac{\partial^2\widehat{g}(\eta,p)}{\partial\eta^2}\right)\frac{\partial^2\widehat{g}(\eta,p)}{\partial\eta^2}-\left(\widehat{f}(\eta,p)+\widehat{g}(\eta,p)\right)\frac{\partial^4\widehat{g}(\eta,p)}{\partial\eta^4}\right], \tag{A.7}$$

$$\begin{aligned}\mathfrak{N}_\theta\left[\widehat{\theta}(\eta,p),\widehat{f}(\eta,p),\widehat{g}(\eta,p),\widehat{\phi}(\eta,p)\right]&=\frac{\partial^2\widehat{\theta}(\eta,p)}{\partial\eta^2}+Pr\left(\widehat{f}(\eta,p)+\widehat{g}(\eta,p)\right)\frac{\partial\widehat{\theta}(\eta,p)}{\partial\eta}\\&-Pr\left(\frac{\partial\widehat{f}(\eta,p)}{\partial\eta}\right)\widehat{\theta}(\eta,p)+Pr.Nb\frac{\partial\widehat{\phi}(\eta,p)}{\partial\eta}\\&\cdot\frac{\partial\widehat{\theta}(\eta,p)}{\partial\eta}+Pr.Nb\left(\frac{\partial\widehat{\theta}(\eta,p)}{\partial\eta}\right)^2,\end{aligned} \tag{A.8}$$

$$\begin{aligned}\mathfrak{N}_\phi\left[\widehat{\phi}(\eta,p),\widehat{f}(\eta,p),\widehat{g}(\eta,p),\widehat{\theta}(\eta,p)\right]&=\frac{\partial^2\widehat{\phi}(\eta,p)}{\partial\eta^2}+Le\left(\widehat{f}(\eta,p)+\widehat{g}(\eta,p)\right)\frac{\partial\widehat{\phi}(\eta,p)}{\partial\eta}\\&-Le\left(\frac{\partial\widehat{f}(\eta,p)}{\partial\eta}\right)\widehat{\phi}(\eta,p)+Sc.\frac{Nt}{Nb}\frac{\partial^2\widehat{\theta}(\eta,p)}{\partial\eta^2},\end{aligned} \tag{A.9}$$

$$\begin{aligned}\mathfrak{N}_N\left[\widehat{N}(\eta,p),\widehat{f}(\eta,p),\widehat{g}(\eta,p),\widehat{\phi}(\eta,p)\right]&=\frac{\partial^2\widehat{N}(\eta,p)}{\partial\eta^2}+Lb\left(\widehat{f}(\eta,p)+\widehat{g}(\eta,p)\right)\frac{\partial\widehat{N}(\eta,p)}{\partial\eta}\\&-Lb\left(\frac{\partial\widehat{f}(\eta,p)}{\partial\eta}\right)\widehat{N}(\eta,p)-Pe.\left[\frac{\partial\widehat{\phi}(\eta,p)}{\partial\eta}\right.\\&\left.+\left(\widehat{N}(\eta,p)+\Omega\right)\frac{\partial^2\widehat{\phi}(\eta,p)}{\partial\eta^2}\right],\end{aligned} \tag{A.10}$$

where $p\in[0,1]$ represents the embedding parameter and h_f, h_g, h_θ, h_ϕ, and h_N are the nonzero auxiliary parameters.

*A.2. **m**th-Order Problem.*

$$\begin{aligned}\mathfrak{L}_f\left[f_m(\eta)-\chi f_{m-1}(\eta)\right]&=h_f\mathfrak{R}_m^f(\eta),\\\mathfrak{L}_g\left[g_m(\eta)-\chi g_{m-1}(\eta)\right]&=h_g\mathfrak{R}_m^g(\eta),\\\mathfrak{L}_\theta\left[\theta_m(\eta)-\chi\theta_{m-1}(\eta)\right]&=h_\theta\mathfrak{R}_m^\theta(\eta),\\\mathfrak{L}_\phi\left[\phi_m(\eta)-\chi\phi_{m-1}(\eta)\right]&=h_\phi\mathfrak{R}_m^\phi(\eta),\\\mathfrak{L}_N\left[N_m(\eta)-\chi N_{m-1}(\eta)\right]&=h_N\mathfrak{R}_m^N(\eta),\end{aligned} \tag{A.11}$$

with

$$\begin{aligned}f_m(0)&=0,\\f_m'(0)&=0,\\f_m'(\infty)&=0,\\g_m(0)&=0,\\g_m'(0)&=0,\\g_m'(\infty)&=0,\\\theta_m(0)&=0,\\\theta_m(\infty)&=0,\\\phi_m(0)&=0,\\\phi_m(\infty)&=0,\\N_m(0)&=0,\\N_m(\infty)&=0,\end{aligned} \tag{A.12}$$

and

$$\begin{aligned}\mathfrak{R}_m^f(\eta)&=f_{m-1}'''+\sum_{k=0}^{m-1}\left(f_{m-1-k}f_k''+g_{m-1-k}f_k''-f_{m-1-k}'f_k'\right)\\&+\beta_1\sum_{k=0}^{m-1}\sum_{l=0}^{k}\left[2\left(f_{m-1-k}f_{k-l}'f_l''+g_{m-1-k}f_{k-l}'f_l''\right)\right.\\&\left.-\left(f_{m-1-k}f_{k-l}f_l'''+g_{m-1-k}g_{k-l}f_l'''+2f_{m-1-k}g_{k-l}f_l'''\right)\right]\\&+\beta_2\sum_{k=0}^{m-1}\sum_{l=0}^{k}\left[2\left(f_{m-1-k}''f_k''+g_{m-1-k}''f_k''\right)\right.\\&\left.-\left(f_{m-1-k}f_k''''+g_{m-1-k}f_k''''\right)\right]+\lambda\left(\theta_{m-1}-Nr\phi_{m-1}\right.\\&\left.-RbN_{m-1}\right),\end{aligned} \tag{A.13}$$

$$\begin{aligned}\mathfrak{R}_m^g(\eta)&=g_{m-1}'''+\sum_{k=0}^{m-1}\left(f_{m-1-k}g_k''+g_{m-1-k}g_k''-g_{m-1-k}'g_k'\right)\\&+\beta_1\sum_{k=0}^{m-1}\sum_{l=0}^{k}\left[2\left(f_{m-1-k}g_{k-l}'g_l''+g_{m-1-k}g_{k-l}'g_l''\right)\right.\\&\left.-\left(f_{m-1-k}f_{k-l}g_l'''+g_{m-1-k}g_{k-l}g_l'''+2f_{m-1-k}g_{k-l}g_l'''\right)\right]\\&+\beta_2\sum_{k=0}^{m-1}\sum_{l=0}^{k}\left[2\left(f_{m-1-k}''g_k''+g_{m-1-k}''g_k''\right)\right.\\&\left.-\left(f_{m-1-k}g_k''''+g_{m-1-k}g_k''''\right)\right],\end{aligned} \tag{A.14}$$

$$\begin{aligned}\mathfrak{R}_m^\theta(\eta)&=\theta_{m-1}''+Pr\sum_{k=0}^{m-1}\left(f_{m-1-k}\theta_k'+g_{m-1-k}\theta_k'-f_{m-1-k}'\theta_k\right.\\&\left.+Nb\theta_{m-1-k}'\phi_k'+Nt\theta_{m-1-k}'\theta_k'\right),\end{aligned} \tag{A.15}$$

$$\begin{aligned}\mathfrak{R}_m^\phi(\eta)&=\phi_{m-1}''+Le\sum_{k=0}^{m-1}\left(f_{m-1-k}\phi_k'+g_{m-1-k}\phi_k'\right.\\&\left.-f_{m-1-k}'\phi_k\right)+\frac{Nt}{Nb}\theta_{m-1}'',\end{aligned} \tag{A.16}$$

$$\begin{aligned}\Re_m^N(\eta) = {} & N_{m-1}'' + Lb\sum_{k=0}^{m-1}\left(f_{m-1-k}N_k' + g_{m-1-k}N_k'\right.\\ & \left. - f_{m-1-k}'N_k - Pe\left(N_{m-1-k}'\phi_k' + N_{m-1-k}\phi_k''\right)\right)\\ & + Pe\Omega\phi_{m-1}'',\end{aligned} \tag{A.17}$$

for $p = 0$ and $p = 1$, and we can write

$$\begin{aligned}\widehat{f}(\eta,0) &= f_0(\eta),\\ \widehat{f}(\eta,1) &= f(\eta),\\ \widehat{g}(\eta,0) &= g_0(\eta),\\ \widehat{g}(\eta,1) &= g(\eta),\\ \widehat{\theta}(\eta,0) &= \theta_0(\eta),\\ \widehat{\theta}(\eta,1) &= \theta(\eta),\\ \widehat{\phi}(\eta,0) &= \phi_0(\eta),\\ \widehat{\phi}(\eta,1) &= \phi(\eta),\\ \widehat{N}(\eta,0) &= N_0(\eta),\\ \widehat{N}(\eta,1) &= N(\eta),\end{aligned} \tag{A.18}$$

when p varies from 0 to 1, $\widehat{f}(\eta,p)$, $\widehat{g}(\eta,p)$, $\widehat{\theta}(\eta,p)$, $\widehat{\phi}(\eta,p)$, and $\widehat{N}(\eta,p)$ vary from the initial solutions $f_0(\eta)$, $g_0(\eta)$, $\theta_0(\eta)$, $\phi_0(\eta)$, and $N_0(\eta)$ to the final solutions $f(\eta)$, $g(\eta)$, $\theta(\eta)$, $\phi(\eta)$ and $N(\eta)$, respectively. By Taylor's series, we have

$$\begin{aligned}\widehat{f}(\eta,p) &= f_0(\eta) + \sum_{m=1}^{\infty} f_m(\eta)\,p^m,\\ f_m(\eta) &= \frac{1}{m!}\left.\frac{\partial^m \widehat{f}(\eta,p)}{\partial p^m}\right|_{p=0},\\ \widehat{g}(\eta,p) &= g_0(\eta) + \sum_{m=1}^{\infty} g_m(\eta)\,p^m,\\ g_m(\eta) &= \frac{1}{m!}\left.\frac{\partial^m \widehat{g}(\eta,p)}{\partial p^m}\right|_{p=0},\\ \widehat{\theta}(\eta,p) &= \theta_0(\eta) + \sum_{m=1}^{\infty} \theta_m(\eta)\,p^m,\\ \theta_m(\eta) &= \frac{1}{m!}\left.\frac{\partial^m \widehat{\theta}(\eta,p)}{\partial p^m}\right|_{p=0},\\ \widehat{\phi}(\eta,p) &= \phi_0(\eta) + \sum_{m=1}^{\infty} \phi_m(\eta)\,p^m,\\ \phi_m(\eta) &= \frac{1}{m!}\left.\frac{\partial^m \widehat{\phi}(\eta,p)}{\partial p^m}\right|_{p=0},\end{aligned}$$

$$\begin{aligned}\widehat{N}(\eta,p) &= N_0(\eta) + \sum_{m=1}^{\infty} N_m(\eta)\,p^m,\\ N_m(\eta) &= \frac{1}{m!}\left.\frac{\partial^m \widehat{N}(\eta,p)}{\partial p^m}\right|_{p=0}.\end{aligned} \tag{A.19}$$

The values of auxiliary parameter are chosen in such a way that the series (A.19) converge at $p = 1$, i.e.,

$$\begin{aligned}f(\eta) &= f_0(\eta) + \sum_{m=1}^{\infty} f_m(\eta),\\ g(\eta) &= g_0(\eta) + \sum_{m=1}^{\infty} g_m(\eta),\\ \theta(\eta) &= \theta_0(\eta) + \sum_{m=1}^{\infty} \theta_m(\eta),\\ \phi(\eta) &= \phi_0(\eta) + \sum_{m=1}^{\infty} \phi_m(\eta),\\ N(\eta) &= N_0(\eta) + \sum_{m=1}^{\infty} N_m(\eta),.\end{aligned} \tag{A.20}$$

The general solutions $(f_m, g_m, \theta_m, \phi_m, N_m)$ of (A.11)-(A.12) in terms of special solutions $(f_m^*, g_m^*, \theta_m^*, \phi_m^*, N_m^*)$ are given by the following:

$$\begin{aligned}f_m(\eta) &= f_m^*(\eta) + A_1 + A_2\exp(\eta) + A_3\exp(-\eta),\\ g_m(\eta) &= g_m^*(\eta) + A_4 + A_5\exp(\eta)\\ &\quad + A_6\exp(-\eta),\\ \theta_m(\eta) &= \theta_m^*(\eta) + A_7\exp(\eta) + A_8\exp(-\eta),\\ \phi_m(\eta) &= \phi_m^*(\eta) + A_9\exp(\eta) + A_{10}\exp(-\eta),\\ N_m(\eta) &= N_m^*(\eta) + A_{11}\exp(\eta) + A_{12}\exp(-\eta),\end{aligned} \tag{A.21}$$

where the constants A_i $(i = 1 - 12)$ through the boundary conditions (A.12) are as follows:

$$\begin{aligned}A_2 &= A_5 = A_7 = A_9 = A_{11} = 0,\\ A_3 &= \left.\frac{\partial f_m^*}{\partial \eta}\right|_{\eta=0},\\ A_1 &= -A_3 - f_m^*(0),\\ A_6 &= \left.\frac{\partial g_m^*}{\partial \eta}\right|_{\eta=0},\\ A_4 &= -A_6 - g_m^*(0),\\ A_8 &= -\theta^*(0),\\ A_{10} &= -\phi^*(0),\\ A_{12} &= -N^*(0).\end{aligned} \tag{A.22}$$

Nomenclature

x, y, z: Dimensional coordinates (m)
T: Nanofluid temperature (K)
u, v, w: Dimensional velocity components (ms^{-1})
C: Nanoparticles volume fraction (−)
n: Number of motile micro-organisms (−)
λ_1: Relaxation time (s)
λ_2: Retardation time (s)
ν: Kinematic viscosity (m^2s^{-1})
ρ_f: Density of nanofluid (kgm^{-3})
ρ_p: Density of nanoparticle (kgm^{-3})
ρ_m: Density of microorganisms particle (kgm^{-3})
T_∞: Ambient fluid temperature (−)
C_∞: Ambient nanoparticles volume fraction (−)
n_∞: Ambient number of motile microorganisms (−)
g: Gravitational acceleration (ms^{-2})
τ: Heat capacity ratio (−)
D_B: Brownian diffusion coefficient (m^2s^{-1})
D_T: Thermophoretic diffusion coefficient (m^2s^{-1})
α_m: Thermal diffusivity of nanofluid (m^2s^{-1})
D_m: Diffusivity of microorganisms (m^2s^{-1})
U_w, V_w: Stretching velocities (ms^{-1})
T_w: Surface temperature (K)
C_w: Surface nanoparticles volume fraction (−)
n_w: Surface number of motile microorganisms (−)
a, b: Stretching rate (ms^{-1})
T_0: Reference temperature (K)
C_0: Reference nanoparticles volume fraction (−)
n_0: Reference number of motile micro-organisms (−)
b_1, d_1, e_1: Constants (−)
η: Dimensionless variable (−)
θ: Dimensionless fluid temperature (−)
ϕ: Dimensionless nanoparticles volume fraction (−)
N: Dimensionless number of motile microorganisms (−)
β_1, β_2: Dimensionless Deborah numbers (−)
λ: Mixed convection parameter (−)
Nr: Buoyancy ratio parameter (−)
Rb: Bioconvection Rayleigh number (−)
Pr: Prandtl number (−)
Nb: Brownian motion parameter (−)
Nt: Thermophoresis motion parameter (−)
Sc: Schmidt number (−)
Lb: Bioconvection Lewis number (−)
Pe: Bioconvection Peclet number (−)
Ω: Micro-organisms concentration difference parameter (−)
α: Stretching ratio parameter (−).

Conflicts of Interest

The authors declare that they have no conflicts of interest.

References

[1] R. G. Larson, *The structure and rheology of complex fluids*, Oxford University Press, New York, NY, USA, 1999.

[2] R. K. Bhatnagar, G. Gupta, and K. R. Rajagopal, "Flow of an Oldroyd-B fluid due to a stretching sheet in the presence of a free stream velocity," *International Journal of Non-Linear Mechanics*, vol. 30, no. 3, pp. 391–405, 1995.

[3] T. Hayat, A. M. Siddiqui, and S. Asghar, "Some simple flows of an Oldroyd-B fluid," *International Journal of Engineering Science*, vol. 39, no. 2, pp. 135–147, 2001.

[4] D. Vieru, C. Fetecau, and C. Fetecau, "Flow of a generalized Oldroyd-B fluid due to a constantly accelerating plate," *Applied Mathematics and Computation*, vol. 201, no. 1-2, pp. 834–842, 2008.

[5] H. Qi and H. Jin, "Unsteady helical flows of a generalized Oldroyd-B fluid with fractional derivative," *Nonlinear Analysis: Real World Applications*, vol. 10, no. 5, pp. 2700–2708, 2009.

[6] M. Jamil, C. Fetecau, and M. Imran, "Unsteady helical flows of Oldroyd-B fluids," *Communications in Nonlinear Science and Numerical Simulation*, vol. 16, no. 3, pp. 1378–1386, 2011.

[7] L. Zheng, Y. Liu, and X. Zhang, "Exact solutions for MHD flow of generalized Oldroyd-B fluid due to an infinite accelerating plate," *Mathematical and Computer Modelling*, vol. 54, no. 1-2, pp. 780–788, 2011.

[8] M. Zhao, S. Wang, and S. Wei, "Transient electro-osmotic flow of Oldroyd-B fluid in a straight pipe of circular cross section," *Journal of Non-Newtonian Fluid Mechanics*, vol. 201, pp. 135–139, 2013.

[9] T. Hayat, T. Hussain, S. A. Shehzad, and A. Alsaedi, "Flow of Oldroyd-B fluid with nanoparticles and thermal radiation," *Applied Mathematics and Mechanics-English Edition*, vol. 36, no. 1, pp. 69–80, 2015.

[10] C. Fetecau and K. Kannan, "A note on an unsteady flow of an Oldroyd-B fluid," *International Journal of Mathematics and Mathematical Sciences*, vol. 19, pp. 3185–3194, 2015.

[11] S. Bariş and M. S. Dokuz, "Three-dimensional stagnation point flow of a second grade fluid towards a moving plate," *International Journal of Engineering Science*, vol. 44, no. 1-2, pp. 49–58, 2006.

[12] P. D. Ariel, "The three-dimensional flow past a stretching sheet and the homotopy perturbation method," *Computers & Mathematics with Applications*, vol. 54, no. 7-8, pp. 920–925, 2007.

[13] T. Hayat and M. Awais, "Three-dimensional flow of upper-convected Maxwell (UCM) fluid," *International Journal for Numerical Methods in Fluids*, vol. 66, no. 7, pp. 875–884, 2011.

[14] S. A. Shehzad, A. Alsaedi, and T. Hayat, "Three-dimensional flow of Jeffery fluid with convective surface boundary conditions," *International Journal of Heat and Mass Transfer*, vol. 55, no. 15-16, pp. 3971–3976, 2012.

[15] S. A. Shehzad, A. Alsaedi, T. Hayat, M. S. Alhuthali, and S. Bhattacharya, "Three-Dimensional Flow of an Oldroyd-B Fluid with Variable Thermal Conductivity and Heat Generation/Absorption," *PLoS ONE*, vol. 8, no. 11, p. e78240, 2013.

[16] W. A. Khan, M. Khan, R. Malik, and M. G. Kuzyk, "Three-Dimensional Flow of an Oldroyd-B Nanofluid towards Stretching Surface with Heat Generation/Absorption," *PLoS ONE*, vol. 9, no. 8, p. e105107, 2014.

[17] M. Ramzan, M. Farooq, M. S. Alhothuali, H. M. Malaikah, W. Cui, and T. Hayat, "Three dimensional flow of an Oldroyd-B fluid with Newtonian heating," *International Journal of Numerical Methods for Heat & Fluid Flow*, vol. 25, no. 1, pp. 68–85, 2015.

[18] B. C. Sakiadis, "Boundary-layer behavior on continuous solid surfaces: I. Boundary-layer equations for two-dimensional and axisymmetric flow," *AIChE Journal*, vol. 7, no. 1, pp. 26–28, 1961.

[19] L. J. Crane, "Flow past a stretching plate," *Zeitschrift für Angewandte Mathematik und Physik (ZAMP)*, vol. 21, no. 4, pp. 645–647, 1970.

[20] A. M. Rashad and S. M. M. El-Kabeir, "Heat and mass transfer in transient flow by mixed convection boundary layer over a stretching sheet embedded in a porous medium with chemically reactive species," *Journal of Porous Media*, vol. 13, no. 1, pp. 75–85, 2010.

[21] N. Sandeep and C. Sulochana, "Momentum and heat transfer behaviour of Jeffrey, Maxwell and Oldroyd-B nanofluids past a stretching surface with non-uniform heat source/sink," *Ain Shams Engineering Journal*, 2016.

[22] H. I. Andersson and B. S. Dandapat, "Flow of a power-law fluid over a stretching sheet," in *Stability Application and Analysis of Continuous Media*, vol. 1, pp. 339–347, 1992.

[23] S. Sharidan, T. Mahmood, and I. Pop, "Similarity solutions for the unsteady boundary layer flow and heat transfer due to a stretching sheet," *International Journal of Applied Mechanics and Engineering*, vol. 11, pp. 647–654, 2006.

[24] T. Hayat, Z. Iqbal, M. Sajid, and K. Vajravelu, "Heat transfer in pipe flow of a Johnson-Segalman fluid," *International Communications in Heat and Mass Transfer*, vol. 35, no. 10, pp. 1297–1301, 2008.

[25] M. Sajid, Z. Abbas, T. Javed, and N. Ali, "Boundary layer flow of an Oldroyd-B fluid in the region of a stagnation point over a stretching sheet," *Canadian Journal of Physiology and Pharmacology*, vol. 88, no. 9, pp. 635–640, 2010.

[26] O. D. Makinde and A. Aziz, "Boundary layer flow of a nanofluid past a stretching sheet with a convective boundary condition," *International Journal of Thermal Sciences*, vol. 50, no. 7, pp. 1326–1332, 2011.

[27] S. Mukhopadhyay and K. Bhattacharyya, "Unsteady flow of a Maxwell fluid over a stretching surface in presence of chemical reaction," *Journal of the Egyptian Mathematical Society*, vol. 20, no. 3, pp. 229–234, 2012.

[28] S. Mukhopadhyay, "Heat transfer analysis for unsteady flow of a Maxwell fluid over a stretching surface in the presence of a heat source/sink," *Chinese Physics Letters*, vol. 29, Article ID 054703, 2012.

[29] S. U. S. Choi and J. A. Eastman, "Enhancing thermal conductivity of fluids with nanoparticles," in *Proceedings of the 1995 ASME International Mechanical Engineering Congress and Exposition*, vol. 66, pp. 99–105, San Franciso, CA, USA, 1995.

[30] J. Buongiorno, "Convective transport in nanofluids," *Journal of Heat Transfer*, vol. 128, no. 3, pp. 240–250, 2006.

[31] M. Mustafa, T. Hayat, and A. Alsaedi, "Unsteady boundary layer flow of nanofluid past an impulsively stretching sheet," *Journal of Mechanics*, vol. 29, no. 3, pp. 423–432, 2012.

[32] S. Shateyi and J. Prakash, "A new numerical approach for MHD laminar boundary layer flow and heat transfer of nanofluids over a moving surface in the presence of thermal radiation," *Boundary Value Problems*, vol. 2014, article 2, 2014.

[33] M. Turkyilmazoglu, "Flow of nanofluid plane wall jet and heat transfer," *European Journal of Mechanics - B/Fluids*, vol. 59, pp. 18–24, 2016.

[34] B. Mahanthesh, B. J. Gireesha, and R. S. Gorla, "Nonlinear radiative heat transfer in MHD three-dimensional flow of water based nanofluid over a non-linearly stretching sheet with convective boundary condition," *Journal of the Nigerian Mathematical Society*, vol. 35, no. 1, pp. 178–198, 2016.

[35] T. J. Pedley, N. A. Hill, and J. O. Kessler, "The growth of bioconvection patterns in a uniform suspension of gyrotactic microorganisms," *Journal of Fluid Mechanics*, vol. 195, pp. 223–237, 1988.

[36] M. J. Uddin, M. N. Kabir, and O. A. Bég, "Computational investigation of Stefan blowing and multiple-slip effects on buoyancy-driven bioconvection nanofluid flow with microorganisms," *International Journal of Heat and Mass Transfer*, vol. 95, pp. 116–130, 2016.

[37] M. J. Uddin, Y. Alginahi, O. A. Beg, and M. N. Kabir, "Numerical solutions for gyrotactic bioconvection in nanofluid-saturated porous media with Stefan blowing and multiple slip effects," *Computers & Mathematics with Applications. An International Journal*, vol. 72, no. 10, pp. 2562–2581, 2016.

[38] N. A. Hill, T. J. Pedley, and J. O. Kessler, "Growth of bioconvection patterns in a suspension of gyrotactic micro-organisms in a layer of finite depth," *Journal of Fluid Mechanics*, vol. 208, pp. 509–543, 1989.

[39] T. J. Pedley and J. O. Kessler, "Hydrodynamic phenomena in suspensions of swimming microorganisms," in *Annual Review of Fluid Mechanics*, vol. 24, pp. 313–358, Annual Reviews, Palo Alto, CA, 1992.

[40] A. J. Hillesdon and T. J. Pedley, "Bioconvection in suspensions of oxytactic bacteria: Linear theory," *Journal of Fluid Mechanics*, vol. 324, pp. 223–259, 1996.

[41] M. Metcalfe and T. J. Pedley, "Falling plumes in bacterial bioconvection," *Journal of Fluid Mechanics*, vol. 445, pp. 121–149, 2001.

[42] N. A. Hill and T. J. Pedley, "Bioconvection," *Japan Society of Fluid Mechanics: Fluid Dynamics Research*, vol. 37, no. 1-2, pp. 1–20, 2005.

[43] Z. Alloui, T. H. Nguyen, and E. Bilgen, "Numerical investigation of thermo-bioconvection in a suspension of gravitactic microorganisms," *International Journal of Heat and Mass Transfer*, vol. 50, no. 7-8, pp. 1435–1441, 2007.

[44] A. A. Avramenko and A. V. Kuznetsov, "The onset of biothermal convection in a suspension of gyrotactic microorganisms in a fluid layer with an inclined temperature gradient," *International Journal of Numerical Methods for Heat & Fluid Flow*, vol. 20, no. 1, pp. 111–129, 2010.

[45] A. Aziz, W. A. Khan, and I. Pop, "Free convection boundary layer flow past a horizontal flat plate embedded in porous medium filled by nanofluid containing gyrotactic microorganisms," *International Journal of Thermal Sciences*, vol. 56, pp. 48–57, 2012.

[46] W. A. Khan, O. D. Makinde, and Z. H. Khan, "MHD boundary layer flow of a nanofluid containing gyrotactic microorganisms past a vertical plate with Navier slip," *International Journal of Heat and Mass Transfer*, vol. 74, pp. 285–291, 2014.

[47] W. A. Khan and O. D. Makinde, "MHD nanofluid bioconvection due to gyrotactic microorganisms over a convectively heat stretching sheet," *International Journal of Thermal Sciences*, vol. 81, no. 1, pp. 118–124, 2014.

[48] S. Siddiqa, M. Sulaiman, M. A. Hossain, S. Islam, and R. S. R. Gorla, "Gyrotactic bioconvection flow of a nanofluid past a vertical wavy surface," *International Journal of Thermal Sciences*, vol. 108, pp. 244–250, 2016.

[49] A. Shafiq, Z. Hammouch, and T. Sindhu, "Bioconvective MHD flow of tangent hyperbolic nanofluid with newtonian heating," *International Journal of Mechanical Sciences*, vol. 133, pp. 759–766, 2017.

[50] A. Alsaedi, M. I. Khan, M. Farooq, N. Gull, and T. Hayat, "Magnetohydrodynamic (MHD) stratified bioconvective flow of nanofluid due to gyrotactic microorganisms," *Advanced Powder Technology*, vol. 28, no. 1, pp. 288–298, 2017.

[51] M. Waqas, T. Hayat, S. A. Shehzad, and A. Alsaedi, "Transport of magnetohydrodynamic nanomaterial in a stratified medium considering gyrotactic microorganisms," *Physica B: Condensed Matter*, vol. 529, pp. 33–40, 2018.

[52] S. J. Liao, *The proposed homotopy analysis technique for the solution of non-linear problems [Ph.D. thesis]*, Shanghai Jiao Tong University, 1992.

[53] S. Liao, "On the homotopy analysis method for nonlinear problems," *Applied Mathematics and Computation*, vol. 147, no. 2, pp. 499–513, 2004.

[54] S. Abbasbandy, "The application of homotopy analysis method to nonlinear equations arising in heat transfer," *Physics Letters A*, vol. 360, no. 1, pp. 109–113, 2006.

[55] M. M. Rashidi, A. M. Siddiqui, and M. Asadi, "Application of Homotopy Analysis Method to the Unsteady Squeezing Flow of a Second-Grade Fluid between Circular Plates," *Mathematical Problems in Engineering*, vol. 2010, Article ID 706840, pp. 1–18, 2010.

[56] T. Hayat, M. Ijaz, S. Qayyum, M. Ayub, and A. Alsaedi, "Mixed convective stagnation point flow of nanofluid with Darcy-Fochheimer relation and partial slip," *Results in Physics*, vol. 9, pp. 771–778, 2018.